

Production and FCNC decay of supersymmetric Higgs bosons into heavy quarks in the LHC

SANTI BÉJAR^{a,b}, JAUME GUASCH^c, JOAN SOLÀ^{c,b}

^a*Grup de Física Teòrica, Universitat Autònoma de Barcelona,
E-08193, Bellaterra, Barcelona, Catalonia, Spain*

^b*Institut de Física d'Altes Energies, Universitat Autònoma de Barcelona,
E-08193, Bellaterra, Barcelona, Catalonia, Spain*

^c*Departament d'Estructura i Constituents de la Matèria, Universitat de Barcelona,
E-08028, Diagonal 647, Barcelona, Catalonia, Spain*

Abstract

We analyze the production and subsequent decay of the neutral MSSM Higgs bosons ($h \equiv h^0, H^0, A^0$) mediated by flavor changing neutral currents (FCNC) in the LHC collider. We have computed the h -production cross-section times the FCNC branching ratio, $\sigma(pp \rightarrow h \rightarrow qq') \equiv \sigma(pp \rightarrow h) \times B(h \rightarrow qq')$, in the LHC focusing on the strongly-interacting FCNC sector. Here qq' is an electrically neutral pair of quarks of different flavors, the dominant modes being those containing a heavy quark: tc or bs . We determine the maximum production rates for each of these modes and identify the relevant regions of the MSSM parameter space, after taking into account the severe restrictions imposed by low energy FCNC processes. The analysis of $\sigma(pp \rightarrow h \rightarrow qq')$ singles out regions of the MSSM parameter space different from those obtained by maximizing only the branching ratio, due to non-trivial correlations between the parameters that maximize/minimize each isolated factor. The production rates for the bs channel can be huge for a FCNC process (0.1 – 1 pb), but its detection can be problematic. The production rates for the tc channel are more modest ($10^{-3} - 10^{-2}$ pb), but its detection should be easier due to the clear-cut top quark signature. A few thousand tc events could be collected in the highest luminosity phase of the LHC, with no counterpart in the SM.

1 Introduction

The search for physics beyond the Standard Model (SM) is a very relevant, if not the most important, endeavor within the big experimental program scheduled for the forthcoming Large Hadron Collider (LHC) experiment at CERN [1, 2]. There are several favorite searching lines on which to concentrate, but undoubtedly the most relevant one (due to its central role in most extensions of the SM) is the physics of the Higgs boson(s) with all its potential physical manifestations. Supersymmetry (SUSY) [3–6] is certainly related to Higgs boson physics, and at the same time it may convey plenty of additional phenomenology. Ever since its inception, SUSY has been one of the most cherished candidates for physics beyond the SM, and as such it will be scrutinized in great detail at the LHC. It is no exaggeration to affirm that the LHC will either prove or disprove the existence of SUSY, at least in its most beloved low-energy realization, namely the one which is needed to solve the longstanding naturalness problem in the Higgs sector of the SM [4]. Indeed, if SUSY is realized around the TeV scale, the LHC experiments shall be able to directly produce the SUSY particles for masses smaller than a few TeV [7, 8]. On the other hand, the presence of SUSY may also be tested indirectly through the quantum effects of the supersymmetric particles. For one thing it has been known since long ago that SUSY particles may produce large virtual effects on Higgs boson observables¹.

Within the general strategy based on detecting indirect effects of the new physics, Flavor Changing Neutral Currents (FCNC) play a very special role. In the SM they are completely absent at the tree-level [23]. At one loop, however, the FCNC effects are possible in the SM, but then the contributions from the new particles enter on equal footing with those from SM particles. Therefore, it is not inconceivable that in certain regions of the parameter space the new physical effects may well dominate the SM contributions, thus providing a unique signature of physics beyond the SM. This is particularly so when the SM one-loop effects, even though non-vanishing, turn out to be highly suppressed. In such situations the sole observation of these FCNC processes would be instant evidence of new physics. A most dramatic example of this kind of appealing scenarios occurs within the FCNC physics of the SM Higgs boson (H_{SM}) interactions with quarks. For example, the FCNC vertex $H_{\text{SM}}tc$ may lead (at one loop) to such rare decays as $t \rightarrow H_{\text{SM}}c$ or $H_{\text{SM}} \rightarrow tc$, depending on the mass of H_{SM} (At the moment both possibilities are still open because the LEP bounds amount to a mass for H_{SM} above 114.4 GeV [24].). Both of these modes are extremely suppressed at one loop, with branching ratios of order 10^{-14} or less, hence 10 orders of magnitude below other more conventional (and relatively well measured) FCNC processes like $b \rightarrow s\gamma$ [24]. The rareness of the FCNC Higgs boson decay modes is borne out by direct calculation [25], and it can also be understood from physical arguments based on dimensional analysis, power counting, CKM matrix elements and dynamical features [26–28]. Therefore, these processes are an ideal laboratory to look for non-standard interactions superimposed onto the SM ones. Similar considerations apply to the FCNC processes associated to the Hbs vertex, but in this case it is more difficult to pin down the phenomenological signatures. Some work along these lines has already

¹See e.g. [9–21] and references therein. For a review see e.g. [22].

been done, both in the MSSM [26, 29–36] and in the general two-Higgs-doublet model (2HDM) [27, 28, 32, 37], and also in other extensions of the SM – see [38] for a review. Up to now, the main effort has been concentrated in computing the FCNC decay modes at one-loop within the new physics, and also in getting a realistic estimate of the maximum branching ratios expected. It is not enough to compute the FCNC branching ratios in, say the MSSM, and then evaluate them in some favorable region of the parameter space, for one has to preserve at the same time the stringent bounds on other observables in which the same physics can be applied, like the aforementioned low-energy $b \rightarrow s\gamma$ decay. This kind of correlated study was done very carefully in Ref. [26] for the specific Higgs boson FCNC decays into bottom quarks within the MSSM, $h \rightarrow b\bar{s}$ ($h = h^0, H^0, A^0$). In this paper we extend the latter work by computing also the top quark Higgs boson FCNC decay modes of the heavy MSSM Higgs bosons, $h \rightarrow t\bar{c}$ ($h = H^0, A^0$) under the same restrictions (recall that h^0 cannot participate in this decay because $m_{h^0} < m_t$ in the MSSM [22]). Furthermore, in this work we carry out an additional step absolutely necessary to make contact with experiment, namely we combine the FCNC decay branching ratios of the MSSM Higgs bosons (into both top and bottom quarks) with their MSSM production cross-sections in order to estimate the maximum number of FCNC events expected at LHC energies and luminosities. Only in this way one can assess in a practical way the probability of detecting such processes at the LHC. While this computation is already in the literature for the general 2HDM [27], to the best of our knowledge the corresponding calculation in the MSSM case is not available. In this paper we perform this calculation and compare the FCNC results obtained for the MSSM and 2HDM scenarios.

The relevant observable quantity on which we shall focus hereafter is the cross-section for the production of electrically neutral pairs of heavy quarks of different flavors at the LHC, whose origin stems from the FCNC decays of the neutral Higgs bosons of the MSSM, $h = h^0, H^0, A^0$ [22, 39]. Thus, we aim at the quantity

$$\begin{aligned} \sigma(pp \rightarrow h \rightarrow qq') &\equiv \sigma(pp \rightarrow hX)B(h \rightarrow qq') \equiv \sigma(pp \rightarrow hX) \frac{\Gamma(h \rightarrow qq')}{\Gamma(h \rightarrow X)} \\ &\equiv \sigma(pp \rightarrow hX) \frac{\Gamma(h \rightarrow q\bar{q}' + \bar{q}q')}{\sum_i \Gamma(h \rightarrow X_i)} \quad (qq' \equiv b\bar{s} \text{ or } t\bar{c}). \end{aligned} \quad (1)$$

Here $\Gamma(h \rightarrow X)$ is the – consistently computed – total width in each case. In order to assess the possibility to measure these processes at the LHC, we have performed a scan of the MSSM parameter space to find the maximum possible value of the production rates (1) under study. The computation of the combined production rate is necessary, since the correlations among the different factors are important. For example, in Ref. [26] it was shown that the maximum branching ratio for the lightest MSSM Higgs boson, $B(h^0 \rightarrow b\bar{s})$, is obtained in the regions of the parameter space where the coupling $h^0 b\bar{b}$ is strongly suppressed by quantum effects. On the other hand, the associated production $\sigma(pp \rightarrow h^0 b\bar{b})$ is one of the leading processes for the production of the lightest MSSM Higgs boson. It is clear then that, in the regions where $B(h^0 \rightarrow b\bar{s})$ is largest, $\sigma(pp \rightarrow h^0 b\bar{b})$ will be suppressed. Therefore, the maximum FCNC production rate at the LHC can only be obtained by the combined analysis of the two relevant factors in (1) (viz. the branching

ratio and the Higgs boson production cross-section). We will see that the effects from each factor are different in different regions of the parameter space. Moreover, the realistic production FCNC rates (1) in the MSSM parameter space can be obtained only by including the restrictions imposed by the simultaneous analysis of the branching ratio of the low-energy process $b \rightarrow s \gamma$, whose range of values is severely limited by experiment [40–45]. As in Ref. [26], in this paper we limit ourselves to supersymmetric FCNC interactions mediated by the strongly interacting sector of the MSSM, i.e. the SUSY-QCD flavor-violating interactions induced by the gluinos. The corresponding analysis for the electroweak supersymmetric FCNC effects requires a lengthy separate presentation, and will be reported elsewhere [46].

The paper is organized as follows. In Section 2 we describe the general setting for our numerical analysis. In Section 3 we present the LHC production rates of Higgs boson decaying into bottom quarks through supersymmetric FCNC interactions. In Section 4 we present the corresponding FCNC rates for the top quark channel. Finally, in Section 5 we compare the MSSM results with the 2HDM results, and deliver our conclusions.

2 General setting for the numerical analysis

To compute the full one-loop value of the FCNC cross-sections $\sigma(pp \rightarrow h \rightarrow q q')$ for the three MSSM Higgs bosons ($h = h^0, H^0, A^0$) we shall closely follow the notation and methods of Refs. [26–29]. We refer the reader to these references for the technical details. In particular, a thorough exposition of the relevant interaction Lagrangians and similar set of Feynman diagrams for the FCNC interactions is provided in [29]. See also [22,39] for basic definitions in the MSSM framework and [11] for detailed computational techniques and further illustration of the supersymmetric enhancement effects in other relevant Higgs boson processes. There is no need to go through these lengthy details here and in what follows we shall limit ourselves to present the final results of our numerical analysis together with a detailed discussion, interpretation and phenomenological application.

We have performed the calculations with the help of the numeric programs HIGLU, PPHTT [47–50] and LoopTools [51–53]. The calculation must obviously be finite without renormalization, and indeed the cancellation of UV divergences using either dimensional regularization or dimensional reduction – the two methods giving the same results here – in the total amplitudes was verified explicitly. In the following we will detail the approximations used in our computation:

- We include the full one-loop SUSY-QCD contributions to the FCNC partial decay widths $\Gamma(h \rightarrow q q')$ in the observable (1).
- We assume that FCNC mixing terms appear only in the LH-chiral sector of the 6×6 squark mixing matrix. Therefore, this matrix has only non-diagonal blocks in the LH-LH sector. This is the most natural assumption from the theoretical point of view [54], and, moreover, it was proven in Ref. [29,32] that the presence of FCNC terms in the RH-chiral sector would enhance the partial widths by a factor two at most – not an order of magnitude.

- The Higgs sector parameters (masses and CP-even mixing angle α) have been treated using the leading m_t and $m_b \tan \beta$ approximation to the one-loop result [55–58]. For comparison, we also perform the analysis using the tree-level approximation.
- The Higgs bosons total decay widths $\Gamma(h \rightarrow X)$ are computed at leading order, including all the relevant channels: $\Gamma(h \rightarrow f\bar{f}, ZZ, W^+W^-, gg)$. The off-shell decays $\Gamma(h \rightarrow ZZ^*, W^\pm W^{\mp*})$ have also been included. This is necessary to consistently compute the total decay width of $\Gamma(h^0 \rightarrow X)$ in regions of the parameter space where the maximization of the cross-section (1) is obtained at the expense of greatly diminishing the partial decay widths of the two-body process $h^0 \rightarrow b\bar{b}$ (due to dramatic quantum effects that may reduce the CP-even mixing angle α to small values [59]). The one-loop decay rate $\Gamma(h \rightarrow gg)$ has been taken from [49] and the off-shell decay partial widths have been recomputed explicitly and found perfect agreement with the old literature on the subject [60].
- The MSSM Higgs boson production cross-sections at the LHC have been computed using the programs HIGLU 2.101 and PPHTT 1.1 [47–50]. These programs include the following channels: gluon-gluon fusion $\sigma(pp(gg) \rightarrow h)$, associated production with top-quarks $\sigma(pp \rightarrow h t\bar{t})$ and associated production with bottom-quarks $\sigma(pp \rightarrow h b\bar{b})$. In order to have a consistent description, we have used the leading order approximation for all channels. The QCD renormalization scale is set to the default values for each program, namely $\mu_0 = m_h$ for HIGLU and $\mu_0 = (m_h + 2M_Q)/2$ for PPHTT. We have used the set of CTEQ4L Parton Distribution Functions [61].

Running quark masses ($m_q(Q)$) and strong coupling constants ($\alpha_s(Q)$) are used throughout, with the renormalization scale set to the decaying Higgs boson mass in the decay processes. More details are given below, as necessary.

Using this setup, we have performed a maximization of the FCNC cross-section, Eq. (1), in the MSSM parameter space with the following restrictions on the parameters:

qq'	bs	tc
δ_{23}	$< 10^{-0.09} \simeq 0.81$	
$\tan \beta$	50	5
A_t	-300 GeV	$ A_t \leq 3M_{\text{SUSY}}$
A_b	$ A_b \leq 3M_{\text{SUSY}}$	300 GeV
μ	$(-1000 \cdots 1000) \text{ GeV}$	
$m_{\tilde{q}_i}$	$m_{\tilde{d}_L} = m_{\tilde{d}_R} = m_{\tilde{u}_R} = m_{\tilde{g}} \equiv M_{\text{SUSY}}$	
M_{SUSY}	$(150 \cdots 1000) \text{ GeV}$	
m_{A^0}	$(100 \cdots 1000) \text{ GeV}$	
$M_{\tilde{q}_i}$	$2 M_{\tilde{q}_i} > m_{H^0} + 50 \text{ GeV}$	
	$M_{\tilde{q}_i} + M_{\tilde{q}_j} > m_{A^0} + 50 \text{ GeV} \ (i \neq j)$	

(2)

Here $m_{\tilde{q}_i}$ are the LH-chiral and RH-chiral squark soft-SUSY-breaking mass parameters, $m_{\tilde{q}_{L,R}}$, common for the three generations; $M_{\tilde{q}_i}$ are the physical masses of the squarks, and

m_h is the mass of the decaying Higgs boson $h = h^0, H^0, A^0$. These masses are fixed at the tree-level by the values of $(\tan \beta, m_{A^0})$ and the SM gauge boson masses and couplings [39]. Due to the structure of the Yukawa couplings in the MSSM, the value of $\tan \beta$ is fixed at a high (small) value for the bottom (top) quark channel as indicated. The parameter m_{A^0} (the mass of the CP-odd Higgs boson) is assumed to vary in the range indicated in (2). At one loop these masses receive corrections from the various SUSY fields, and therefore depend on the values of the remaining parameters in Eq. (2). The characteristic SUSY mass scale M_{SUSY} defines the typical mass of the squark and gluino masses². The rest of the parameters of the squark sector are determined by this setup. For instance, by $SU(2)$ gauge invariance we have $m_{\tilde{u}_L} = m_{\tilde{d}_L}$. Following the same notation as in [29], the parameter δ_{23} represents the mixing between the second and third generation of LH-chiral squarks. Let us recall its definition:

$$\delta_{23} \equiv \frac{m_{\tilde{b}_L \tilde{s}_L}^2}{m_{\tilde{b}_L} m_{\tilde{s}_L}}, \quad (3)$$

$m_{\tilde{b}_L \tilde{s}_L}^2$ being the non-diagonal term in the squark mass matrix squared mixing the second and third generation of LH-chiral squarks – and an equivalent definition for the up-type quarks.³ The parameter δ_{23} is a fundamental quantity in our analysis as it determines the strength of the tree-level FCNC interactions induced by the supersymmetric strong interactions, which are then transferred to the loop diagrams of the Higgs boson FCNC decays in Eq. (1). The last two restrictions in Eq. (2) ensure that the (heavy) Higgs boson decay channels into a pair of squarks are kinematically forbidden. We have checked explicitly for some of the heavy Higgs boson channels (h^0 can never do it in practice) that we obtain the same results if we remove these conditions and include the partial widths $\Gamma(h \rightarrow \tilde{q}\tilde{q}^*)$ in the denominator of (1). Strictly speaking this condition could be implemented, in the case of the H^0 boson, by just requiring $m_{H^0} < 2 M_{\tilde{q}_i}$, but we have made it stronger by including an additive term. This term is arbitrary (provided it is not very small) and acts as a buffer, namely it impedes that by an appropriate choice of the squark masses we can approach arbitrarily close the threshold from above, and therefore avoids artificial enhancement effects in our loop calculations (see below). Similarly, for the CP-odd Higgs boson, the condition expressed in (2) ensures that we avoid a similar kind of enhancement. In this case, however, the condition is a bit different because the $A^0 \tilde{q}\tilde{q}^*$ vertex can only exist with squarks of different chirality types ($A^0 \tilde{q}_L \tilde{q}_R^*$) or, equivalently, with different mass eigenstates ($A^0 \tilde{q}_i \tilde{q}_j^*$). We have used fixed values for the soft-SUSY-breaking trilinear couplings A_t and A_b for the bs and tc channels respectively. Our results are essentially independent of these values and their signs.

The task of scanning the MSSM parameter space in order to maximize $\sigma(pp \rightarrow h \rightarrow qq')$ for the various Higgs bosons is quite demanding and highly CPU-time consuming,

²Our programs are able to deal with completely arbitrary masses for each squark, but we are forced to make some simplifications in order to provide a reasonable analysis within a manageable total CPU time, see below.

³Recall that the δ_{ij} parameters in the up-sector are related to the corresponding parameters in the down-sector by the Cabibbo-Kobayashi-Maskawa matrix, see e.g. [62, 63].

even under the conditions imposed in Eq. (2). As stated in the introduction, our code includes also the restrictions on the MSSM parameter space due to the experimental constraint on $B(b \rightarrow s\gamma)$, and therefore contains the full one-loop SUSY-QCD amplitude for $b \rightarrow s\gamma$ constructed from the FCNC interactions induced by the gluinos. The scan was carried out with the help of two entirely different methods. In the first method we used a systematic procedure based on dividing the parameter subspace (2) into a lattice which we filled with points distributed in a completely homogeneous way. The second is a Monte-Carlo based method, first proposed in [64]. We have adapted the well-known Vegas integration program [65] to generate a sufficient number of “interesting” points in our parameter subspace. The total number of points used in this case was far smaller than in the first method. Obviously the lattice procedure gives more accurate results by increasing arbitrarily the total number of points, but the CPU time becomes prohibitively long for the whole analysis. This is so even after factoring out in a suitable way the phase-space integrals of the Higgs boson production processes, so that these integrals are computed only once for every fixed Higgs boson mass and for all the MSSM points of our scan in the parameter subspace (2). The second method is comparatively much faster, but it still involves a quite respectable amount of CPU time for the whole analysis. We found that the partial results obtained by the two methods are compatible at the level of 10 – 20%. For the study of our FCNC processes we consider that this level of accuracy should be acceptable, and for this reason all of the plots that we present in this work have been finally computed with the Vegas-based procedure. This also explains the wiggling appearance observed in the profiles of the curves presented in Sections 3-4. For any given abscissa point in each one of these curves, the corresponding value on the vertical (ordinate) axis is somewhere within a band whose width lies around 10 – 20% of the central value.

A few words on the effects of the $B(b \rightarrow s\gamma)$ constraint in our analysis are now in order. The SUSY-QCD contribution to $B(b \rightarrow s\gamma)$ can be quite large, in fact as large as the SM one, and with any sign. This raises the possibility of “fine-tuning” between the two type of contributions in certain (narrow) regions of the parameter space. As a consequence we could highly optimize our FCNC rates in these regions without being in conflict with the experimentally measured $B(b \rightarrow s\gamma)$ band. We have checked that in these regions the number of FCNC events can be artificially augmented by one or two orders of magnitude. Our scanning procedure indeed finds automatically these fine-tuning domains. However, we have systematically avoided them in the presentation of our analysis (for more details cf. [26]). In all of our plots, therefore, we show the results obtained for the non-fine-tuned case only. We adopt $B(b \rightarrow s\gamma) = (2.1 - 4.5) \times 10^{-4}$ as the experimentally allowed range within three standard deviations [24].

3 Analysis of the bottom-strange channel

The main result of the numerical scan for the bottom channel is shown in Fig. 1. To be specific: Fig. 1a shows the maximum values of the production cross-sections $\sigma(pp \rightarrow$

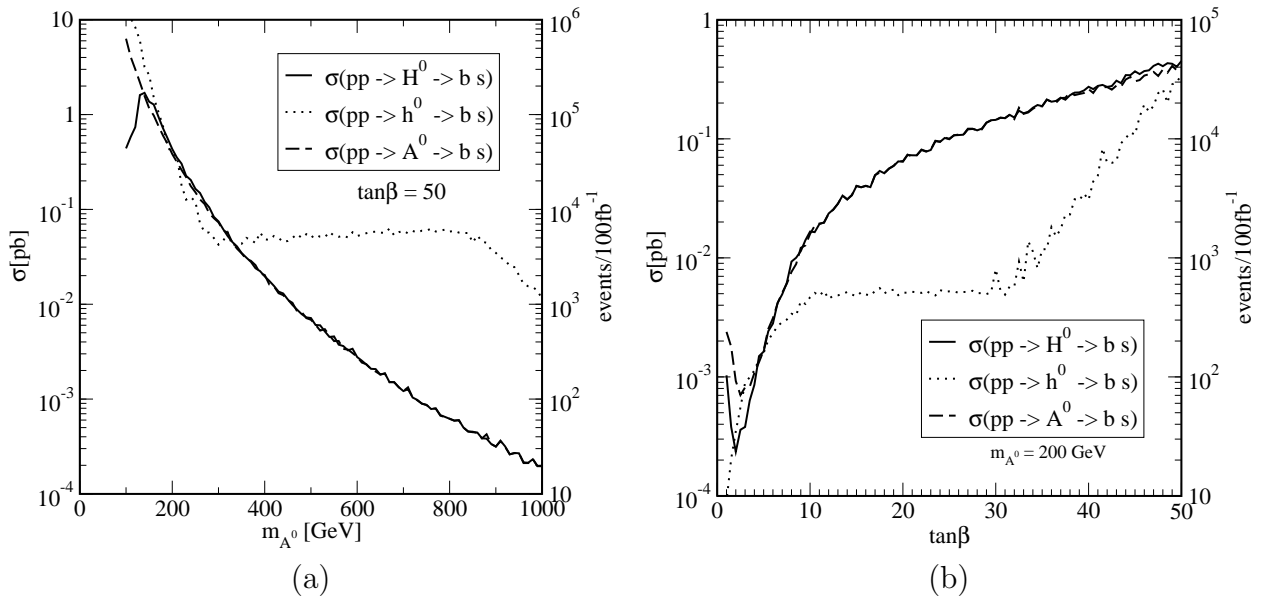


Figure 1: Maximum SUSY-QCD contributions to $\sigma(pp \rightarrow h \rightarrow b s)$, Eq. (1), as a function of **(a)** m_{A^0} (at fixed $\tan \beta$) and **(b)** $\tan \beta$ (at fixed m_{A^0}). In each plot the left-vertical axis provides the cross-section in pb and the right-vertical axis tracks the number of events per 100 fb^{-1} of integrated luminosity.

$h \rightarrow b s$) for the three MSSM Higgs bosons $h = h^0, H^0, A^0$ at the LHC, as a function of m_{A^0} ; Fig. 1b displays the cross-section as a function of $\tan \beta$. In this plot we indicate the value of $\sigma(pp \rightarrow h \rightarrow b s)$ (in pb) in the left-vertical axis, and at the same time we track number of FCNC events (per 100 fb^{-1} of integrated luminosity) on the right vertical axis. Looking at Fig. 1 one can see immediately that at large $\tan \beta$: i) the maximum number of events is remarkably high (10^6 events!) for a FCNC process; ii) there is a sustained region in the h^0 channel, comprising the interval $300 \text{ GeV} \lesssim m_{A^0} \lesssim 900 \text{ GeV}$, with a flat value of 5×10^3 events; iii) the chosen value of $\tan \beta = 50$ is not critical for H^0 and A^0 as long it is larger than 10. In Fig. 1b we see that the dependence on $\tan \beta$ is essentially the same for H^0 and A^0 , but for h^0 it is quite different: in the region $10 \lesssim \tan \beta \lesssim 30$ the cross-section remains below 10^{-2} pb, but for $\tan \beta > 30$ it starts climbing fast up to 0.3 pb at $\tan \beta = 50$. The number of events here reaches a few times 10^4 for all channels (for fixed $m_{A^0} = 200 \text{ GeV}$)⁴. For further reference, in Table 1 we show the numerical values of $\sigma(pp \rightarrow h \rightarrow b s)$ together with the parameters which maximize the production for $\tan \beta = 50$ and $m_{A^0} = 200 \text{ GeV}$. We include the value of $B(h \rightarrow b s)$ at the maximization point of the FCNC cross-section. We notice that at this point the lightest Higgs boson h^0 is the one having the smallest branching ratio. This is in contrast to the situation when one maximizes the branching ratios independently of the number of events [26].

In Fig. 2a we show the effect on $\sigma(pp \rightarrow h^0 \rightarrow b s)$, and on the total decay width $\Gamma(h^0 \rightarrow X)$, of using the Higgs boson sector at the tree-level or at one-loop in our computation. It is well-known that the h^0 couplings to quarks are particularly sensitive to

⁴As already advertised, in reading the plots and tables in this work, one must keep in mind that they are the result of a Monte-Carlo sampling near the region of the maximal values.

h	H^0	h^0	A^0
$\sigma(pp \rightarrow h \rightarrow bs)$	0.45 pb	0.34 pb	0.37 pb
events/100 fb $^{-1}$	4.5×10^4	3.4×10^4	3.7×10^4
$B(h \rightarrow bs)$	9.3×10^{-4}	2.1×10^{-4}	8.9×10^{-4}
$\Gamma(h \rightarrow X)$	10.9 GeV	1.00 GeV	11.3 GeV
δ_{23}	$10^{-0.62}$	$10^{-1.32}$	$10^{-0.44}$
$m_{\tilde{q}}$	990 GeV	670 GeV	990 GeV
A_b	-2750 GeV	-1960 GeV	-2860 GeV
μ	-720 GeV	-990 GeV	-460 GeV
$B(b \rightarrow s\gamma)$	4.50×10^{-4}	4.47×10^{-4}	4.39×10^{-4}

Table 1: Maximum value of $\sigma(pp \rightarrow h \rightarrow bs)$ (and of the number of bs events per 100 fb^{-1}) in the LHC, for $m_{A^0} = 200$ GeV and $\tan\beta = 50$. Shown are also the corresponding values of the relevant branching ratio $B(h \rightarrow bs)$ and of the total width of the Higgs bosons, together with the values of the SUSY parameters. The last row includes $B(b \rightarrow s\gamma)$.

this issue, and for this reason we focus on the lightest CP-even Higgs boson for these considerations. We can appreciate the correlations among the different factors that enter the production rate (1). The plotted values for $\sigma(pp \rightarrow h^0 \rightarrow bs)$ and $\Gamma(h^0 \rightarrow X)$ in Fig. 2a correspond precisely to the parameters that maximize (1) at the tree-level or at one loop in each case. Fig. 2b shows a comparison of the various h^0 -production mechanisms for the values that maximize $\sigma(pp \rightarrow h^0 \rightarrow bs)$ at one-loop. Remarkably, the effect of the radiative corrections in the Higgs sector amounts to an enhancement of our maximal FCNC rates of up to three orders of magnitude. As we mentioned in the introduction (see also Ref. [26]) the maximum of $B(h^0 \rightarrow b\bar{s})$ is attained under the conditions of the so-called “small α_{eff} scenario” [59, 66], where the two-body decay $h^0 \rightarrow b\bar{b}$ is strongly suppressed due to a corresponding suppression of the $h^0 b\bar{b}$ coupling. Since $\Gamma(h^0 \rightarrow b\bar{b})$ usually dominates the total width $\Gamma(h^0 \rightarrow X)$, the latter also diminishes drastically (at the level of the partial width of a h^0 three-body decay, as mentioned above). In this scenario the production cross-section $\sigma(pp \rightarrow h^0 b\bar{b})$ is also suppressed, so the final result is a compromise between the suppression of $\Gamma(h^0 \rightarrow b\bar{b})$ and the possible enhancement (or at least sustenance) of $\sigma(pp \rightarrow h^0 X)$ by other mechanisms other than the associated production with bottom quarks (like the mechanism of gluon-gluon fusion, see Fig. 2b).

Indeed, for $m_{A^0} \lesssim 300$ GeV we can check in Fig. 2b that the most relevant factor for maximizing the FCNC cross-section is the enhancement of the h^0 production channel in association with bottom quarks, $\sigma(pp \rightarrow h^0 b\bar{b})$. This channel operates through the $b\bar{b}$ -fusion vertex $b\bar{b} \rightarrow h^0$ and is highly enhanced at large $\tan\beta$. In the region $m_{A^0} \lesssim 300$ GeV stays as the dominant mechanism for h^0 production, although one can see that the alternate gg -fusion mechanism remains all the way non-negligible. The corresponding effect on our FCNC cross-section (1) is nevertheless not obvious because this same parameter choice does also maximize the total width of h^0 , mainly through the enhancement of $\Gamma(h^0 \rightarrow b\bar{b})$. There is a delicate interplay of various factors here. In particular, in the region $m_{A^0} < 300$ GeV the maximized partial width of the FCNC process $h^0 \rightarrow bs$ (which is a function of all the parameters in (2)) is larger than in the region $m_{A^0} > 300$ GeV,

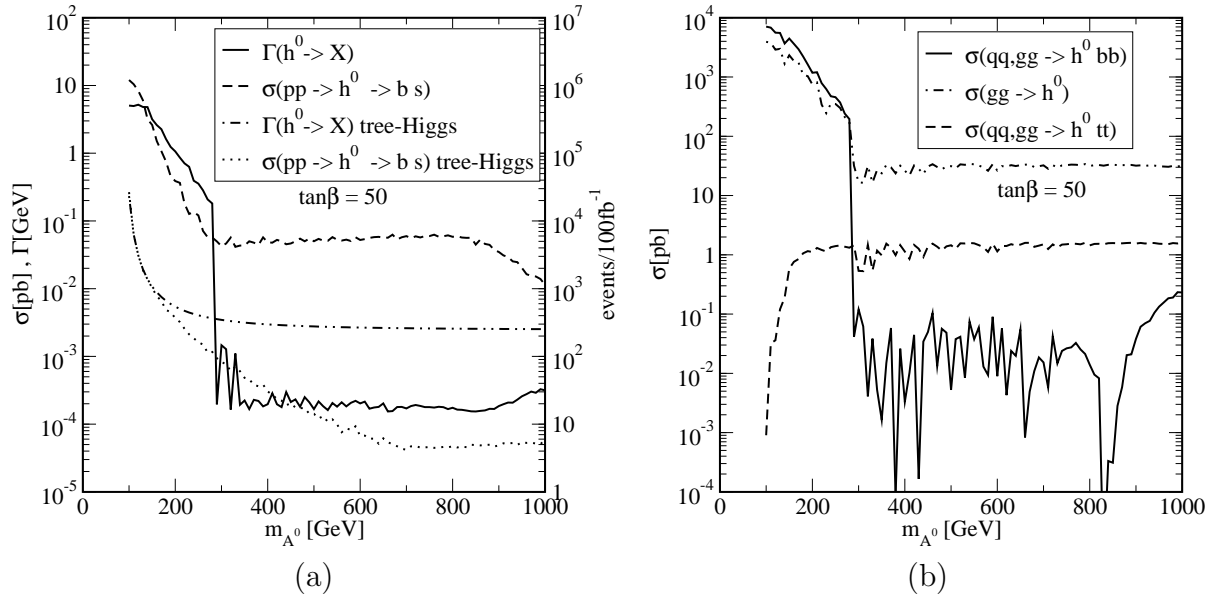


Figure 2: **(a)** h^0 production cross-section and decay width as a function of m_{A^0} with the Higgs mass relations at tree-level and at one-loop. **(b)** Different contributions to the h^0 production cross-section as a function of m_{A^0} corresponding to the maximization of $\sigma(pp \rightarrow h^0 \rightarrow b s)$ using the one-loop Higgs mass relations.

but at the same time the total width becomes smaller in the latter region. Overall, the result is that $\sigma(pp \rightarrow h^0 \rightarrow b s)$ is larger in the former m_{A^0} range than in the latter. Furthermore, when we cross ahead the limit $m_{A^0} \simeq 300$ GeV the dominant h^0 -production channel changes turn: the associated h^0 -production with bottom quarks falls abruptly down (see explanations below) and the gluon-gluon fusion mechanism takes over, so that in this range the h^0 -production cross-section becomes completely dominated by $gg \rightarrow h^0$. We note that while this mechanism is not so efficient at its maximum as the associated production, it has a virtue: it is non-suppressed in the entire range of m_{A^0} . As a result, in the region above $m_{A^0} \gtrsim 300$ GeV a small value of the $h^0 b\bar{b}$ coupling enhances $B(h^0 \rightarrow b s)$ while it does not dramatically suppress the total cross-section $\sigma(pp \rightarrow h X)$. For $m_{A^0} > 300$ GeV our sampling procedure finds the maximum by selecting the points in parameter space corresponding to the small α_{eff} scenario, where $B(h^0 \rightarrow b s)$ takes the highest values and $\Gamma(h^0 \rightarrow X)$ and $\sigma(pp \rightarrow h^0 b\bar{b})$ are strongly suppressed – the latter staying below the associated Higgs boson production with top quarks! In this way the net Higgs boson cross-section $\sigma(pp \rightarrow h^0)$ is not drastically reduced thanks to the sustenance provided by the gg -fusion channel. Most of the loop contributions to it come from the top quark because the bottom quark contribution is suppressed and the squarks are rather heavy. One can clearly see this sustenance feature in Fig. 2 in the form of a long cross-section plateau up to around $m_{A^0} = 1$ TeV, beyond which the small α_{eff} scenario cannot be maintained and $\Gamma(h^0 \rightarrow X)$ starts increasing and at the same time $\sigma(pp \rightarrow h^0 \rightarrow b s)$ starts decreasing. It is remarkable that this behavior is only feasible thanks to the large radiative corrections in the MSSM Higgs sector. When we, instead, perform the computation using the tree-level relations for the Higgs sector, the small α_{eff} scenario is obviously

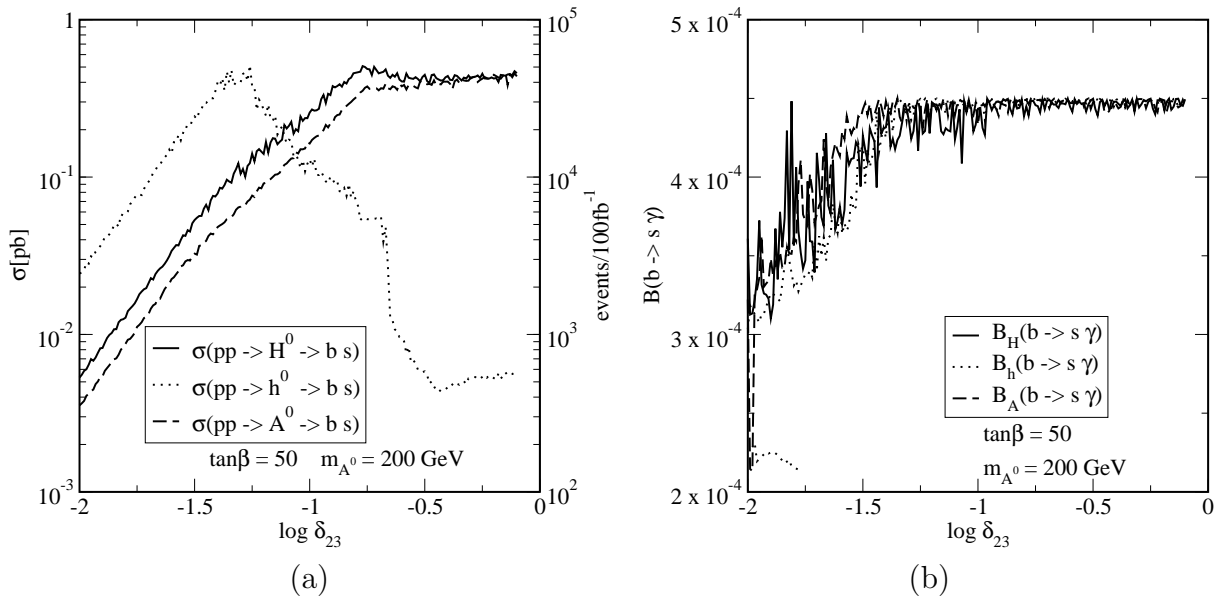


Figure 3: Maximum SUSY-QCD contributions to $\sigma(pp \rightarrow h \rightarrow b s)$, Eq. (1), as a function of (a) δ_{23} and (b) value of $b \rightarrow s\gamma$.

not possible and the enhancements/suppressions of $\sigma(pp \rightarrow h^0 b \bar{b})/\Gamma(h^0 \rightarrow X)$ cannot take place. As a result the FCNC rate is some 3 orders of magnitude smaller than in the previous case.

Next, we turn our attention to the FCNC mixing parameter δ_{23} in Eq. (3). The value of δ_{23} at the cross-section maximum is not necessarily the maximum allowed value of δ_{23} in (2). This is because it is a conditioned maximum, namely a maximum obtained under the restrictions imposed by $b \rightarrow s\gamma$, as illustrated in Fig. 3. For further reference in our discussion, and to better grasp some qualitative features of our results, let us write the general form of the SUSY-QCD contribution to $b \rightarrow s\gamma$. If we emphasize only the relevant supersymmetric terms under consideration (obviating the powers of the gauge couplings and other factors) we have

$$B(b \rightarrow s\gamma) \sim \delta_{23}^2 \frac{m_b^2 (\mu - A_b \tan\beta)^2}{M_{\text{SUSY}}^4}. \quad (4)$$

Fig. 3a shows the maximum of $\sigma(pp \rightarrow h \rightarrow b s)$ as a function of δ_{23} for a fixed value of the CP-odd Higgs boson mass $m_{A^0} = 200$ GeV, whereas Fig. 3b shows the computed value of $B(b \rightarrow s\gamma)$ corresponding to the parameter space points where each maximum is attained. At small δ_{23} the SUSY-QCD contribution to $B(b \rightarrow s\gamma)$ is negligible, and the experimental restriction $B(b \rightarrow s\gamma) = (2.1 - 4.5) \times 10^{-4}$ does not place constraints on the other MSSM parameters (2); in other words, in this region the dependence is $\sigma(pp \rightarrow h \rightarrow b s) \propto (\delta_{23})^2$ – the naively expected one. Here $\delta_{23} \lesssim 10^{-1.5} \simeq 0.03$ and the computed $B(b \rightarrow s\gamma)$ value lies well within the experimental limit. For larger δ_{23} , $B(b \rightarrow s\gamma)$ can be saturated at its uppermost experimentally allowed limit, and the rest of the parameters in (2) must change accordingly in order not to cross that limit. This can be appreciated in Fig. 4 where we

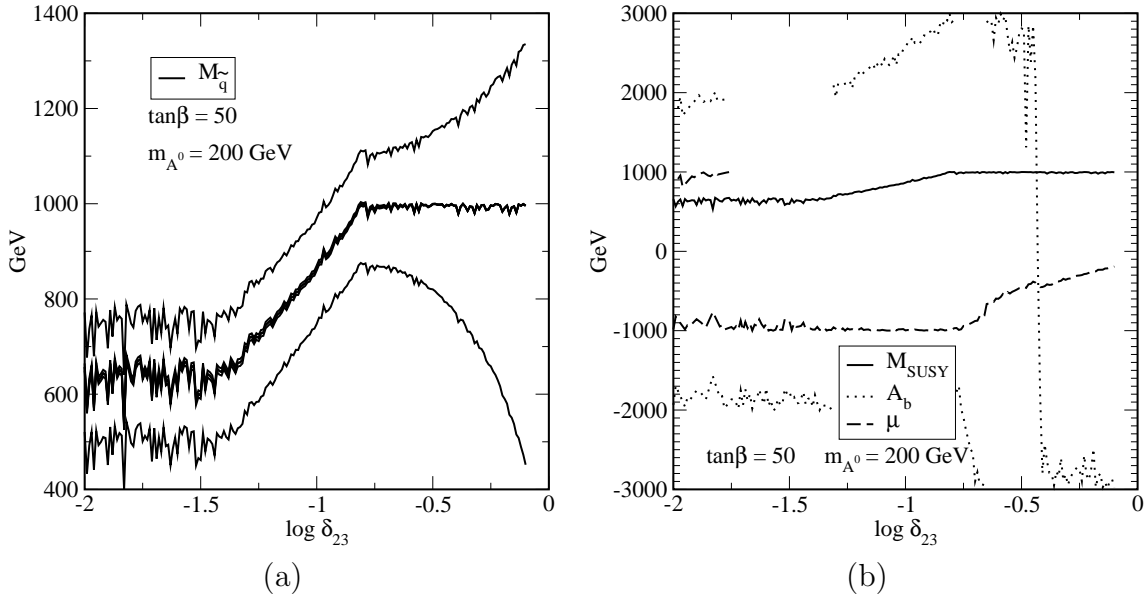


Figure 4: Value of **(a)** down-type squark physical masses ($M_{\tilde{q}}$), four of them are degenerate; **(b)** the parameters (2) from the maximization of the h^0 channel in Fig. 3a.

show the range of values taken by the physical down-type squark masses⁵ (Fig. 4a) and the lagrangian parameters (Fig. 4b) from Eq. (2) that provide the maximum values of $\sigma(pp \rightarrow h^0 \rightarrow bs)$ in Fig. 3. In the small δ_{23} region ($\delta_{23} \lesssim 10^{-1.5} \simeq 0.03$) the parameters and masses that maximize $\sigma(pp \rightarrow h \rightarrow bs)$ are constant – except for the statistical noise unavoidable in a Monte-Carlo procedure. Note also that there are two possible values for the parameters μ and A_b , due to the fact that (the leading contribution of) $\sigma(pp \rightarrow h \rightarrow bs)$ is independent of the sign of these parameters and the Monte-Carlo procedure picks either sign for each point with equal probability. At $\delta_{23} \simeq 10^{-1.5}$ the value of $B(b \rightarrow s\gamma)$ becomes saturated and $\sigma(pp \rightarrow h^0 \rightarrow bs)$ reaches its maximum (cf. Fig. 3b); however δ_{23} can keep growing, yet without overshooting the $B(b \rightarrow s\gamma)$ limits, because the increasing value of δ_{23} is compensated by the growing squark masses (cf. Fig. 4a). But this is not all that simple, the higher range of δ_{23} can be further divided in two more segments where different dynamical features occur. In the first range, namely $10^{-1.5} \lesssim \delta_{23} \lesssim 10^{-0.75}$, the heavy Higgs boson channels keep on increasing their FCNC rates, but not so the lightest Higgs boson channel $\sigma(pp \rightarrow h^0 \rightarrow bs)$, the reason being that for higher squark masses we reach the region where the small α_{eff} scenario is feasible and hence the h^0 couplings become weakened. The relevant terms of the cross-section can roughly be written as follows (see Ref. [26]):

$$\sigma(pp \rightarrow h^0 \rightarrow bs) \sim \sigma(pp \rightarrow h^0) \times \delta_{23}^2 \cos^2(\beta - \alpha_{\text{eff}}) m_{\tilde{g}}^2 \mu^2 / M_{\text{SUSY}}^4, \quad (5)$$

so that for large $\tan\beta$ and small α_{eff} it becomes reduced. In the second high range of δ_{23} , i.e. for $\delta_{23} \gtrsim 10^{-0.75} \simeq 0.18$, the SUSY mass parameter M_{SUSY} has already reached

⁵There are six different down-type squarks, but four of them are nearly degenerate in mass in our approximation. For the bs -channel, the down squarks are so heavy that the conditions required in the last two rows of (2) are automatically satisfied by them in practically all the allowed range for m_{A^0} .

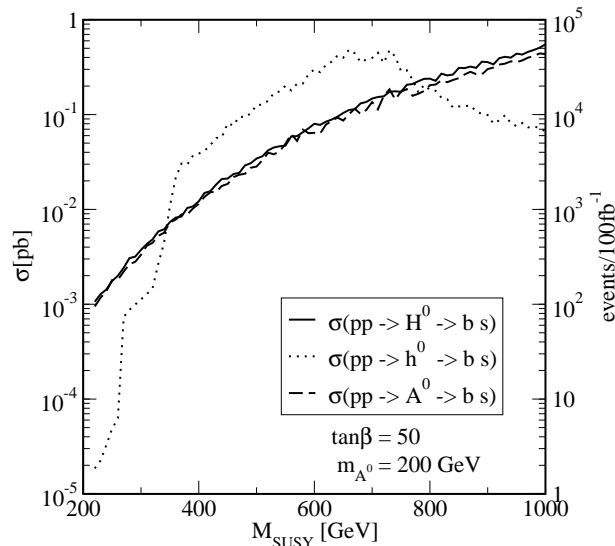


Figure 5: Maximum SUSY-QCD contributions to $\sigma(pp \rightarrow h \rightarrow b s)$, Eq. (1), as a function of M_{SUSY} .

its allowed maximum value specified in (2), therefore other parameters have to change to compensate for the larger δ_{23} . This is confirmed in Fig. 4b, where for $\delta_{23} \gtrsim 10^{-0.75}$ the absolute value of μ decreases to preserve the $B(b \rightarrow s\gamma)$ upper bound. Correspondingly, in this region $\sigma(pp \rightarrow h^0 \rightarrow b s)$ further falls down, as it is patent in Fig 3a. This additional feature can also be understood from the approximate expression of the cross-section given above. At the same time the FCNC rates for $h = H^0, A^0$ keep further growing, but at a much lower pace. This is because their (approximate) contribution goes like

$$\sigma(pp \rightarrow (H^0, A^0) \rightarrow bs) \sim \sigma(pp \rightarrow H^0, A^0) \times \delta_{23}^2 (\sin^2(\beta - \alpha_{\text{eff}}), 1) m_{\tilde{g}}^2 \mu^2 / M_{\text{SUSY}}^4, \quad (6)$$

similar to the h^0 case but with angular dependences on α_{eff} and β which are non-suppressing in this region (see Ref. [26])⁶. Again, any further increase of δ_{23} is now partially cancelled by the $b \rightarrow s\gamma$ constraint, which demands smaller values of μ . This explains the stabilization of the FCNC rates of the H^0 and A^0 channels in the highest δ_{23} range (cf. Fig. 3a). The profile of the squark mass curves in Fig. 4a implies a mixing mass matrix with constant diagonal terms (with value M_{SUSY}) and growing mixing terms (δ_{23}).

We finish our analysis of $\sigma(pp \rightarrow h \rightarrow b s)$ by looking at its behavior as a function of the SUSY mass scale M_{SUSY} , viz. the overall scale for the squark and gluino masses – cf. Eq. (2). Fig. 5 shows the maximum of $\sigma(pp \rightarrow h \rightarrow b s)$ as a function of M_{SUSY} for fixed $m_{A^0} = 200$ GeV and $\tan \beta = 50$. The interpretation of this figure follows closely the results of the previous ones. At small values of M_{SUSY} the potentially large contribution to $B(b \rightarrow s\gamma)$ has to be compensated – see Eq. (4) – by small values of δ_{23} and/or $|\mu|$, resulting in a (relatively) small value of $\sigma(pp \rightarrow h \rightarrow b s)$. As M_{SUSY} grows, δ_{23} and $|\mu|$ can take larger values without disturbing the restrictions from $B(b \rightarrow s\gamma)$. The leading contribution to our FCNC cross-sections is actually independent of the overall SUSY mass

⁶In Eq.(6) above we have corrected a typing mistake present in Eq. (3.5) of Ref. [26].

scale M_{SUSY} , because for all Higgs boson channels we have found the general behavior (leaving aside other terms mentioned above)

$$\sigma(pp \rightarrow h \rightarrow b s) \sim \sigma(pp \rightarrow h) \times \delta_{23}^2 m_g^2 \mu^2 / M_{\text{SUSY}}^4 \quad (h = h^0, H^0, A^0). \quad (7)$$

The last factor effectively behaves as $\delta_{23}^2 \mu^2 / M_{\text{SUSY}}^2$, and grows as δ_{23}^2 for increasing M_{SUSY} at fixed ratio μ / M_{SUSY} . Under the same conditions $B(b \rightarrow s \gamma)$ causes no problem because it is additionally suppressed by $m_b^2 / M_{\text{SUSY}}^2$ – cf. Eq. (4). Therefore, we are led to a sort of “non-decoupling behavior” of the FCNC rates with increasing M_{SUSY} . In other words, we find that for the heavy neutral Higgs bosons (H^0, A^0) the interesting region is (contrary to naive expectations) the high M_{SUSY} range! The lightest Higgs boson (h^0) channel shows a similar overall behavior, but it presents additional features because it is more tied to the evolution of the CP-even mixing angle α . The most interesting region for this channel is (cf. Fig. 5) the central squark mass scale $M_{\text{SUSY}} \sim 600 - 800$ GeV, where the small α_{eff} scenario can take place.

From the combined analysis of Figs. 1-5 we arrive at the following conclusions concerning the bs final state:

- A significant event rate of FCNC Higgs boson decays $\sigma(pp \rightarrow h \rightarrow b s)$ is expected at the LHC, even after taking into account the limits on $B(b \rightarrow s \gamma)$;
- Lightest Higgs boson case, h^0 :
 - For $m_{A^0} \lesssim 300$ GeV the rate $\sigma(pp \rightarrow h^0 \rightarrow b s)$ decreases with m_{A^0} but it is the largest in this interval, being produced by the combination of a large production cross-section $\sigma(pp \rightarrow h^0 b \bar{b})$ and a moderate $B(h^0 \rightarrow b s)$. It amounts to a number of events between $\sim 5 \times 10^3$ and $\sim 12 \times 10^5$ for every 100 fb^{-1} of integrated luminosity at the LHC;
 - For $300 \text{ GeV} \lesssim m_{A^0} \lesssim 850 \text{ GeV}$ we expect a maximum of $\sim 6 \times 10^3$ events/ 100 fb^{-1} in the small α_{eff} scenario, provided by a large $B(h^0 \rightarrow b s)$ and $\sigma(pp(gg) \rightarrow h^0)$ as the dominant production cross-section;
 - For $m_{A^0} > 850$ GeV the number of events starts to decrease slowly;
 - In all cases, this maximum is attained for a large value of $\tan \beta \sim 50$, a moderate value of the SUSY mass scale ($M_{\text{SUSY}} \sim 600 - 800$ GeV) and a *low* value of $\delta_{23} \sim 10^{-1.3} \sim 0.05$;
- Heavy Higgs bosons, H^0, A^0 :
 - Although not shown in our plots, we have checked that their production rate $\sigma(pp \rightarrow H^0, A^0)$ decreases fast with the Higgs boson mass (due to the decreasing of the production cross-section). We find a maximum FCNC rate of $\sim 5 \times 10^4$ events for $m_{A^0} \simeq 200$ GeV, and 20 events for $m_{A^0} \simeq 1$ TeV.
 - The maximum is produced at i) large $\tan \beta > 30$, ii) at the highest allowed values of the SUSY mass scale, $M_{\text{SUSY}} \sim 1$ TeV, and iii) at a relatively large

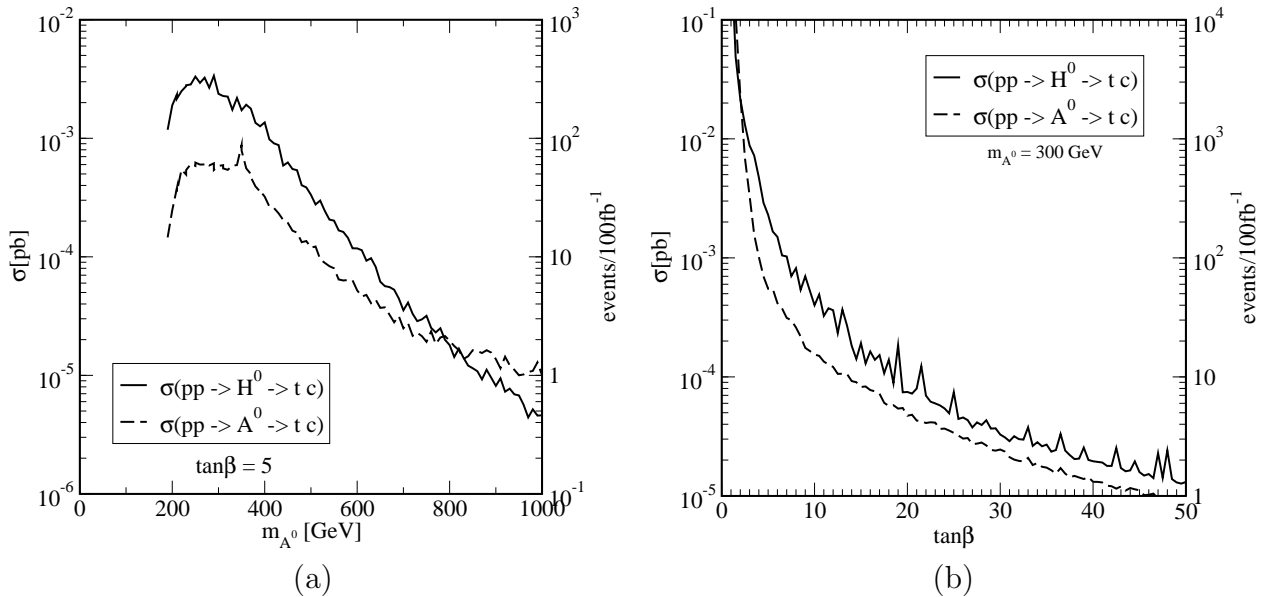


Figure 6: Maximum SUSY-QCD contributions to $\sigma(pp \rightarrow h \rightarrow tc)$, Eq. (1), as a function of (a) m_{A^0} (at fixed $\tan\beta$) and (b) $\tan\beta$ (at fixed m_{A^0}).

value of the FCNC mixing parameter, $\delta_{23} \sim 10^{-0.75} \sim 0.18$, but not at the largest allowed value. The small α_{eff} scenario plays no role in the heavy Higgs boson channels.

Altogether one should expect a total maximum of some 120,000 events/100 fb $^{-1}$.

4 Analysis of the top-charm channel

The results of the numerical scan for this channel are similar to the bs channel, so we will focus mainly on the differences. Fig. 6a shows the maximum value of the production cross-section $\sigma(pp \rightarrow h \rightarrow tc)$, Eq. (1), under study as a function of m_{A^0} ; Fig. 6b displays the cross-section as a function of $\tan\beta$. Obviously the lightest Higgs boson (h^0) channel does not appear in these plots, since in the MSSM this boson is always lighter than the top quark. Looking at Fig. 6 one can see immediately the following: i) the dominant channel in this case is the heavy scalar Higgs boson, H^0 ; ii) it varies between 1 and 300 events/100 fb $^{-1}$; iii) the $\tan\beta$ value is critical with preference for low values. In Table 2 we show the numerical values of $\sigma(pp \rightarrow h \rightarrow tc)$ together with the parameters which maximize the production for $\tan\beta = 5$ and $m_{A^0} = 300$ GeV. We have included the value of $B(h \rightarrow tc)$ at the maximization point of the FCNC cross-section. It is remarkable that for the heavy CP-even Higgs boson one can reach $B(H^0 \rightarrow tc) \sim 10^{-3}$ compatible with the $b \rightarrow s\gamma$ constraint.

Let us remark that for the heavy Higgs boson channels the features of the small α_{eff} scenario play no significant role because the partial widths into $b\bar{b}$ are proportional either to $\cos^2 \alpha_{\text{eff}}$ (in the H^0 case) or to $\sin^2 \beta$ (A^0 case). Moreover, in the low $\tan\beta \gtrsim 1$ region (the relevant allowed one for the tc channel) the small α_{eff} scenario does not even have a

h	H^0	A^0
$\sigma(pp \rightarrow h \rightarrow tc)$	2.4×10^{-3} pb	5.8×10^{-4} pb
events/100 fb $^{-1}$	240	58
$B(h \rightarrow tc)$	1.9×10^{-3}	5.7×10^{-4}
$\Gamma(h \rightarrow X)$	0.41 GeV	0.39 GeV
δ_{23}	$10^{-0.10}$	$10^{-0.13}$
$m_{\tilde{q}}$	880 GeV	850 GeV
A_t	-2590 GeV	2410 GeV
μ	-700 GeV	-930 GeV
$B(b \rightarrow s\gamma)$	4.13×10^{-4}	4.47×10^{-4}

Table 2: Maximum value of $\sigma(pp \rightarrow h \rightarrow tc)$ (and of the number of tc events per 100 fb^{-1}) in the LHC, for $m_{A^0} = 300$ GeV and $\tan\beta = 5$. Shown are also the corresponding values of the relevant branching ratio $B(h \rightarrow tc)$ and of the total width of the Higgs bosons, together with the values of the SUSY parameters. The last row includes $B(b \rightarrow s\gamma)$.

chance to take place.

We turn now our view to the role of the $B(b \rightarrow s\gamma)$ restriction in Figs. 7 and 8. Fig. 7 shows the maximum value of $\sigma(pp \rightarrow h \rightarrow tc)$ as a function of δ_{23} for a fixed value of $m_{A^0} = 300$ GeV together with the corresponding computed value of $B(b \rightarrow s\gamma)$, while Fig. 8 shows the values of the parameters, Eq. (2), that realize this maximum, together with the physical up-type squark masses. In this case the $B(b \rightarrow s\gamma)$ restriction is not as critical as in the bs channel, in part due to the fact that the SUSY-QCD contribution to $B(b \rightarrow s\gamma)$ is not enhanced at low $\tan\beta$. For $\delta_{23} \lesssim 10^{-1.5}$ the value of $B(b \rightarrow s\gamma)$ is well inside the experimental limits (Fig. 7b), there is no restriction on the rest parameters (Fig. 8b), the squark masses remain constant (Fig. 8a), and the maximum value of $\sigma(pp \rightarrow h \rightarrow tc)$ grows here in the naively expected way $(\delta_{23})^2$ (Fig. 7a). Above this value ($\delta_{23} \gtrsim 10^{-1.5}$) the parameters have to be adjusted to provide an acceptable range for $B(b \rightarrow s\gamma)$ ⁷. In this region the SUSY mass M_{SUSY} grows (Fig. 8b), and $|\mu|$ decreases, but not so fast as in the bs channel case (Fig. 4b). At the same time A_t increases with increasing $\delta_{23} > 10^{-1.5}$. Most of the physical squark masses grow, but one of the up-type squarks (stop squark) can always have the minimum allowed mass – Eq. (2). In this region the observables under study grow more slowly, since their original δ_{23}^2 behavior is partially cancelled by the growing of M_{SUSY} with δ_{23} . In Fig. 9 we see, again, that $\sigma(pp \rightarrow h \rightarrow tc)$ grows with the SUSY mass scale (although in a way less pronounced than in the bs channel), due to the relaxation of the $b \rightarrow s\gamma$ constraint for large M_{SUSY} . While $\sigma(pp \rightarrow h \rightarrow bs)$ is augmented nearly three orders of magnitude in the range $M_{\text{SUSY}} = 200 - 1000$ GeV (Fig. 5), the tc channel undergoes only an increase of roughly a factor 10 in the same parameter range.

How do the two Higgs boson channels H^0 and A^0 compare as sources of tc events? The gg -fusion mechanism is one of the leading processes for Higgs boson production at

⁷The two lines appearing in this region for $B_H(b \rightarrow s\gamma)$ mean that the maximum of $\sigma(pp \rightarrow H^0 \rightarrow tc)$ is attained either by the maximum or the minimum allowed value of $B(b \rightarrow s\gamma)$, our Monte-Carlo sampling procedure picks either choice with equal probability for each value of δ_{23} .

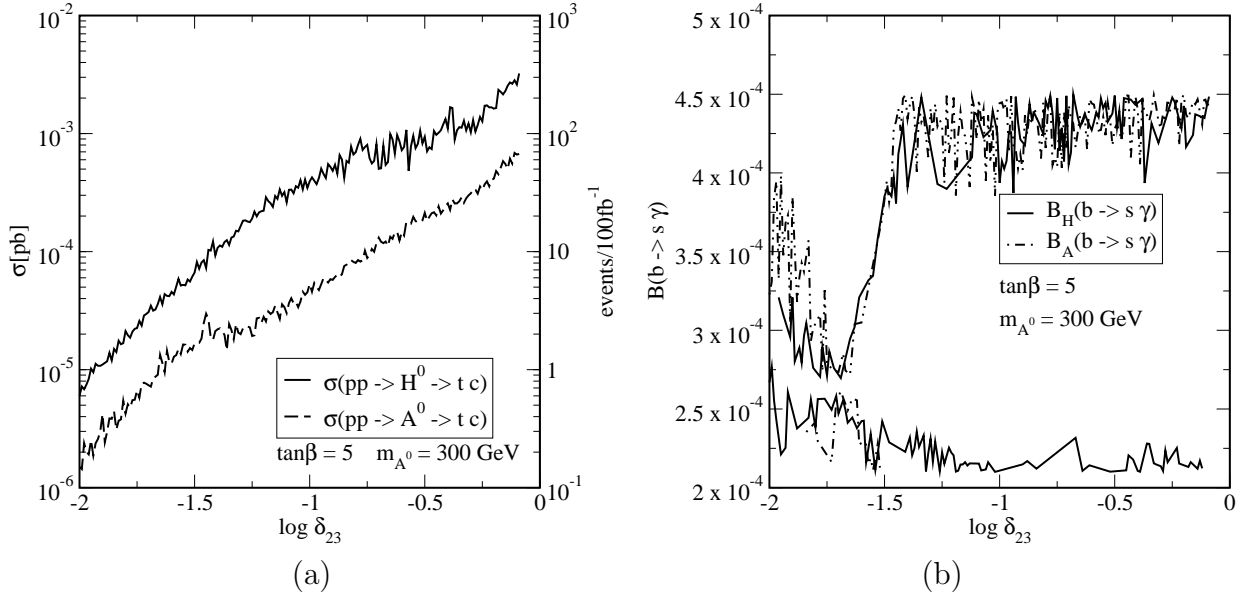


Figure 7: Maximum SUSY-QCD contributions to $\sigma(pp \rightarrow h \rightarrow tc)$, Eq. (1), as a function of (a) δ_{23} and (b) value of $b \rightarrow s\gamma$, for fixed $\tan\beta$ and m_{A^0} .

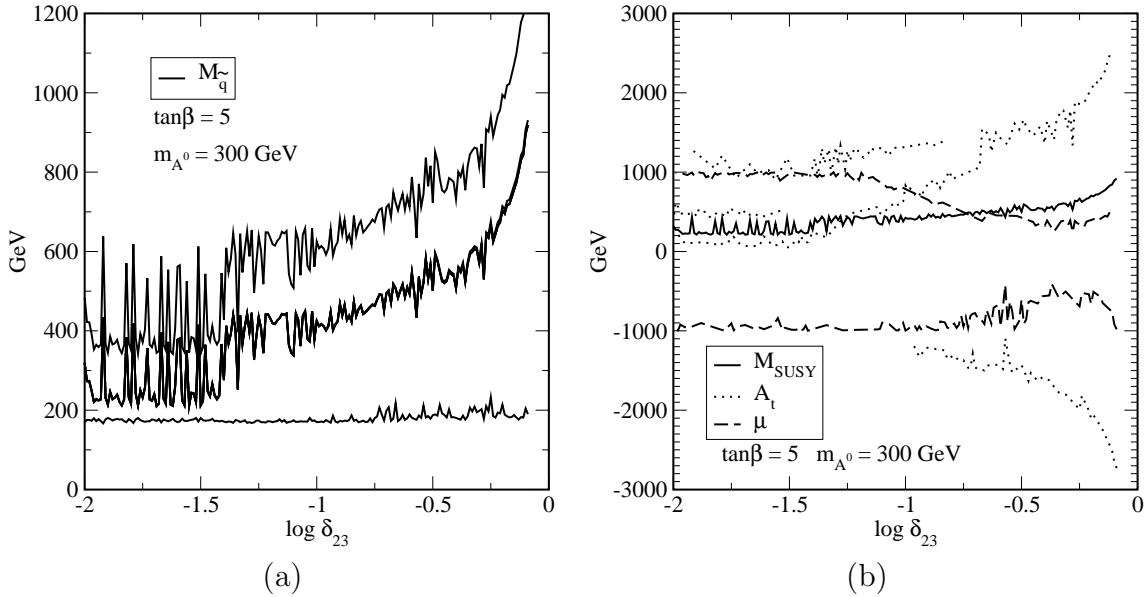


Figure 8: Value of (a) up-type squark physical masses ($M_{\tilde{q}}$), four of them are degenerate; (b) the parameters (2) from the maximization of the H^0 channel in Fig. 7a.

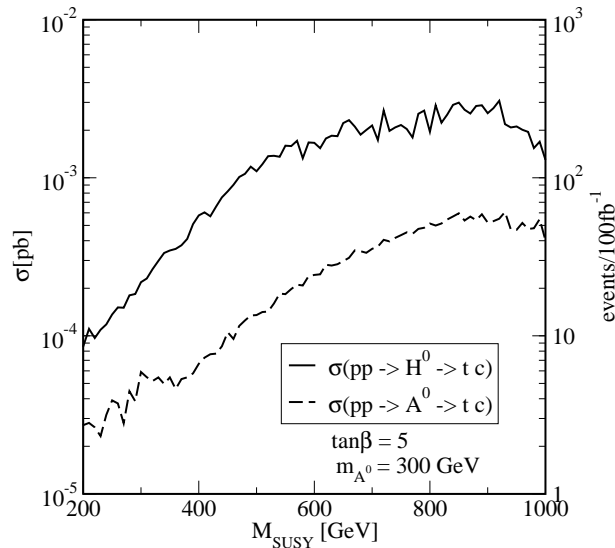


Figure 9: Maximum SUSY-QCD contributions to $\sigma(pp \rightarrow h \rightarrow tc)$, Eq. (1), as a function of M_{SUSY} .

relatively small values of $\tan \beta \gtrsim 1$ – associated production with $b\bar{b}$ remaining still sizeable. Due to CP conservation, the squark contributions to $gg \rightarrow A^0$ cancel out at one-loop and only the quark contributions remain [50]. For large squark masses the production cross-sections for H^0 and A^0 are similar, the latter being slightly larger. We see from Fig. 6 that, despite the similarity in production, the H^0 channel gives larger FCNC rates than the A^0 one. The excess of FCNC events from the former can be explained mainly from the constraints that we have imposed from the very beginning on the squarks masses in relation to the Higgs boson masses (see Eq. (2)). As we have noted in section 2, we can have squarks of the same chirality-type in the $H^0 \tilde{q}\tilde{q}^*$ vertex, whereas they must necessarily be of opposite chirality-type in the $A^0 \tilde{q}\tilde{q}^*$ case. As a result, for small m_{A^0} the squark mass constraints expressed in (2) allow the FCNC cross-section maximization process to pick points near the saturation of the mass condition $2M_{\tilde{q}_i} > m_{H^0} + 50 \text{ GeV}$, but not of $M_{\tilde{q}_i} + M_{\tilde{q}_j} > m_{A^0} + 50 \text{ GeV}$ for ($i \neq j$) because only one of the up-squarks can be light (see Fig. 8a). This produces an enhancement of the branching ratio of $H^0 \rightarrow tc$ and for this reason this FCNC channel dominates in the relatively small m_{A^0} region. However, as soon as m_{A^0} is sufficiently heavy the second mass constraint can also be satisfied and then the two curves in Fig. 6 tend to converge.

From the combined analysis of Figs. 6-9, we conclude that in the case of the H^0 channel we expect a maximum of ~ 300 events/100 fb $^{-1}$ decays into top quarks at the LHC. This maximum is achieved for a CP-odd Higgs boson mass of $m_{A^0} \sim 300 \text{ GeV}$, and a moderately low $\tan \beta \sim 5$. This rate can grow one order of magnitude by a lower value of $\tan \beta \sim 2$, but decreases significantly with m_{A^0} . The maximum is obtained at the largest possible value of δ_{23} , and a moderate SUSY mass scale $M_{\text{SUSY}} \sim 600 - 800 \text{ GeV}$, but having one of the squarks light. While the number of events is significantly lower than the bs -channel ones, the tc -channels offers a better opportunity for detection, due to the much lower background.

5 Discussion and conclusions

We have carried out a systematic study of the production rate of FCNC processes at the LHC mediated by the decay of neutral Higgs bosons of the MSSM: $\sigma(pp \rightarrow h \rightarrow qq')$ ($h = h^0, H^0, A^0$) – see Eq. (1). Specifically, we have concentrated on the FCNC production of the heavy quark pairs $qq' = bs$ and tc , because they are the only ones that have a chance of being detected. We have focused on the FCNC supersymmetric effects stemming from the strongly interacting sector of the MSSM, namely from the gluino-mediated flavor-changing interactions. We have performed a maximization of the event rates in the parameter space under a set of conditions that can be considered “irreducible”, see Eq. (2), i.e. we cannot further shorten this minimal set (e.g. by making additional assumptions on the relations among the parameters) without potentially jeopardizing the conclusions of this study. Even within this restricted parameter subspace the computer analysis has been rather demanding. The numerical scan has been performed using Monte Carlo techniques which we have partially cross-checked with more conventional methods. The maximization of the cross-sections (1) has been performed by simultaneously computing the corresponding MSSM quantum effects on the (relatively well-measured) low-energy FCNC decay $b \rightarrow s\gamma$ and requiring that the experimental limits on this observable are preserved.

To summarize our results: the total number of FCNC heavy flavor events originating from supersymmetric Higgs boson interactions at the LHC can be large (of order 10^6), but this does not mean that they can be easily disentangled from the underlying background of QCD jets where they are immersed. For example, it is well known that the simple two-body decay $h \rightarrow b\bar{b}$ is impossible to isolate due to the huge irreducible QCD background from $b\bar{b}$ dijets – a result that holds for both the SM and the MSSM [1, 2]. This led a long time ago to complement the search with many other channels, particularly $h \rightarrow \gamma\gamma$ which has been identified as an excellent signature in the appropriate range. Similarly, the FCNC Higgs boson decay channels may help to complement the general Higgs boson search strategies, mainly because the FCNC processes should be essentially free of QCD background. Notwithstanding other difficulties can appear, such as misidentification of jets. For instance, for the bs final states misidentification of b -quarks as c -quarks in cs -production from charged currents may obscure the possibility that the bs -events can be really attributed to Higgs boson FCNC decays. This also applies to the tc final states, where misidentification of b -quarks as c -quarks in e.g. tb production might be a source of background to the tc events, although in this case the clear-cut top quark signature should be much more helpful (specially after an appropriate study of the distribution of the signal versus the background). However, to rate the actual impact of these disturbing effects one would need an additional study which is beyond the scope of the present paper.

An interesting (and counter-intuitive) result of our work is that for all the Higgs boson channels $h = h^0, H^0, A^0$, the FCNC cross-section $\sigma(pp \rightarrow h \rightarrow qq')$ increases with growing SUSY mass scale M_{SUSY} . Due to this effective “non-decoupling” behavior (which is more pronounced for the bs channel) the FCNC rates are maximal when the overall squark and gluino mass scale is of order of $M_{\text{SUSY}} \lesssim 1 \text{ TeV}$ – with the only proviso that for the tc -channel a single squark should have a low mass ($\gtrsim 150 \text{ GeV}$). Moreover, we find

that the two types of FCNC final states (bs and tc) prefer different ranges of $\tan\beta$. The bs -channel is most efficient at high $\tan\beta > 30$, whereas the tc -channel works better in the regime of low $\tan\beta < 10$ (see below). As for the mixing parameter δ_{23} (which is the fundamental supersymmetric FCNC parameter of our analysis, see its definition in (3)) we remark that the maximum number of events is not always attained for the largest possible values of it (due to the influence of the $b \rightarrow s\gamma$ constraint): in the bs -channel the maximum is achieved for moderate values in the range $0.05 \lesssim \delta_{23} \lesssim 0.2$, whereas the tc -channel prefers the maximum allowed values in our analysis ($\delta_{23} \lesssim 0.8$). We also remark that the naive expectation $\sigma(pp \rightarrow h \rightarrow qq') \sim \delta_{23}^2$ does not always apply.

The number of FCNC events originating from the two channels bs and tc is not alike, and it also depends on the particular Higgs boson. For the bs final states we have found that the optimized value of $\sigma(pp \rightarrow h \rightarrow bs)$ produced by our analysis is ~ 12 pb. This amounts to $\sim 12 \times 10^5$ events per $\int \mathcal{L} dt = 100 \text{ fb}^{-1}$ of data at the LHC. The most favorable Higgs boson channel is the one corresponding to the lightest MSSM Higgs boson, h^0 . For this boson there are non-trivial correlations between the two factors in Eq. (1), namely between the Higgs boson production cross-section and the FCNC branching ratio. These correlations permit an increase of the total number of FCNC events up to two orders of magnitude in certain cases as compared to the number of events produced by the heavy Higgs bosons H^0 and A^0 , which are essentially free of these correlations. The latter stem from relevant quantum effects on the parameters of the Higgs boson sector at one-loop precisely in the regions of our interest.

On the other hand, the maximum value of $\sigma(pp \rightarrow h \rightarrow tc)$ is more moderate, to wit: 3×10^{-3} pb, or ~ 300 events/ 100 fb^{-1} . For the total integrated luminosity during the operative lifetime of the LHC, which amounts to some $(300 - 400) \text{ fb}^{-1}$, we estimate that a few thousand tc events could be collected in the most optimistic conditions. This number is of course sensitive to many MSSM parameters, but most particularly to two: m_{A^0} and $\tan\beta$. The mass of the CP-odd Higgs boson should not be heavier than $m_{A^0} \sim (400 - 500) \text{ GeV}$ if one does not want to decrease the number of events below a few hundred per 100 fb^{-1} . On the other hand the number of events is very much dependent on the particular range of $\tan\beta$. As we have said above, the lowest possible values are preferred for the tc channel, but the sensitivity in this range is so high that the order of magnitude of $\sigma(pp \rightarrow h \rightarrow tc)$ may change for different (close) choices of $\tan\beta$. Throughout all the analysis of the tc channel we have fixed $\tan\beta$ at an intermediate value, but the maximum number of events per 100 fb^{-1} would grow from ~ 300 (for our standard choice $\tan\beta = 5$) up to $\sim (500, 900, 2000)$ if we would have chosen $\tan\beta = (4, 3, 2)$ respectively. Such lower values of $\tan\beta$ are usually avoided in some MSSM analyses in the literature, but as a matter of fact there are no fully water-tight experimental bounds on $\tan\beta$ excluding this lower range, apart from the more incontrovertible strict lowest limit $\tan\beta > 1$. We recall that the lower limit on $\tan\beta$ is obtained indirectly from the LEP exclusion data on the light Higgs boson search, and is therefore very sensitive to the inputs used in the computation, specially the top quark mass [67]. Unlike the difficulties in the bs -channel, and in spite of the substantially smaller number of events, we deem more feasible to extract the tc signal at the LHC, due to the presence of the quark top, which carries a

highly distinguishable signature.

At this point a comparison with our previous work [27] is in order. In that work we have studied in quite some detail the maximum FCNC production rates of Higgs bosons decaying into tc final states within the general two-Higgs-doublet model. It was found that the maximal branching ratio in the 2HDM takes place in the type II 2HDM (or 2HDM II), and reads $B^{II}(h \rightarrow tc) \sim 10^{-5}$, whereas in the 2HDM I it is comparatively negligible. After a detailed computation of the event rates (including also the particular restrictions of the $b \rightarrow s\gamma$ process, which are different in the 2HDM case as compared to the MSSM) the conclusion was that several hundred tc events could be collected at the LHC under optimal conditions. We clearly identified which are the most relevant Higgs boson modes for this purpose and the domains of the 2HDM II parameter space where these events could originate from. To make it short, our conclusion there [27] was that the h^0 is the most gifted decay and the ideal situation occurs when $\tan\beta$ and $\tan\alpha$ are both large, and also when the CP-odd state A^0 is much heavier than the CP-even ones (h^0, H^0). Furthermore we found that in the general 2HDM the A^0 state never gives any appreciable FCNC rate into tc . It is easy to see that the mode $A^0 \rightarrow bs$ is not favored either (unless $\tan\beta$ is very small and m_{H^\pm} unusually light, both situations rather unappealing).

How it compares with the MSSM case under study? To start with, we note that here the A^0 channel gives essentially the same bs rate as the H^0 one, and that both modes can be quite relevant. At the same time the A^0 rate into tc is, though not dominant, not negligible at all. Some few hundred events of this nature per 100 fb^{-1} are possible. If this is not enough, in the MSSM the most relevant $\tan\beta$ region for the tc final states is not the highest one (as in the 2HDM II case) but just the opposite: the lowest allowed one. This is an important difference, and one that should help to discriminate between the 2HDM and MSSM models in case that some tc events would be unambiguously tagged at the LHC. After all there are many high precision observables that are highly sensitive to the preferred range of $\tan\beta$, so that the favorite value of $\tan\beta$ could already be fixed from other experiments by the time that some FCNC events could be detected. Apart from the different correlation of the parameters in the non-supersymmetric and supersymmetric model, in the latter case the maximal event rates for the tc mode are typically one order of magnitude higher than the maximal event rates in the former.

The corresponding study for the 2HDM branching ratios into bs final states was performed in [37], although in this work the cross-section and number of events were not computed. However, from the maximum size of the expected branching ratios compatible with $b \rightarrow s\gamma$ (viz. $B^{II}(h \rightarrow bs) \sim 10^{-6} - 10^{-5}$ in the 2HDM II) it is already pretty obvious that the number of events can never be competitive with the supersymmetric case where $B^{MSSM}(h \rightarrow bs) \sim 10^{-4} - 10^{-3}$ [26]. As for the 2HDM I (which is insensitive to the $b \rightarrow s\gamma$ bounds) the branching ratios can be at most of order $B^I(h \rightarrow bs) \sim 10^{-5} - 10^{-3}$ and only so for very small values of $\tan\beta = 0.1 - 0.5$ which are actually excluded in the MSSM.

Summing up and closing: the maximum number of FCNC events in the MSSM case is larger than the highest expected rates both in the 2HDM I and II, the two kind of signatures of physics beyond the SM being perfectly distinguishable because the relevant

regions of the parameter space are completely different. If a sample of FCNC events of this kind could be collected, we should be able to ascertain which is its ultimate origin. At the end of the day if one single thing should be emphasized is that the FCNC event rate into bs or tc is so extremely tiny in the SM that if only a dozen events of this kind could be captured under suitable experimental conditions it would be an undeniable signature of new physics. From what we have seen, the odds should be heavily in favor of attributing it to a supersymmetric origin.

Acknowledgements

The work of SB has been supported by CICYT under project FPA2002-00648, by the EU network on Supersymmetry and the Early Universe (HPRN-CT-2000-00152), and by DURSI Generalitat de Catalunya under project 2001SGR-00188; JG by a *Ramon y Cajal* contract from MEC (Spain); JG and JS in part by MEC and FEDER under project 2004-04582-C02-01, and JS also by DURSI Generalitat de Catalunya under project 2001SGR-00065.

References

- [1] ATLAS Collaboration, CERN/LHCC/94-43, Atlas Technical Design Report.
- [2] CMS Collaboration, CERN/LHCC/94-38, CMS Technical Proposal.
- [3] H. P. Nilles, Phys. Rept. **110**, 1 (1984).
- [4] H. E. Haber and G. L. Kane, Phys. Rept. **117**, 75 (1985).
- [5] A. B. Lahanas and D. V. Nanopoulos, Phys. Rept. **145**, 1 (1987).
- [6] S. Ferrara, editor, *Supersymmetry*, volume 1-2, North Holland/World Scientific, Singapore, 1987.
- [7] G. Weiglein et al. (LHC/LC Study Group Collaboration), (2004), hep-ph/0410364.
- [8] G. Degrassi et al., Acta Phys. Polon. **B35**, 2711–2726 (2004).
- [9] J. Guasch, R. A. Jiménez and J. Solà, Phys. Lett. **B360**, 47–56 (1995), hep-ph/9507461.
- [10] J. A. Coarasa, R. A. Jiménez and J. Solà, Phys. Lett. **B389**, 312–320 (1996), hep-ph/9511402.
- [11] J. A. Coarasa, D. Garcia, J. Guasch, R. A. Jiménez and J. Solà, Eur. Phys. J. **C2**, 373–392 (1998), hep-ph/9607485.
- [12] J. Guasch and J. Solà, Phys. Lett. **B416**, 353–360 (1998), hep-ph/9707535.

- [13] J. A. Coarasa, D. Garcia, J. Guasch, R. A. Jiménez and J. Solà, Phys. Lett. **B425**, 329–336 (1998), [hep-ph/9711472](#).
- [14] J. A. Coarasa, J. Guasch and J. Solà, 4th Int. Symposium on Radiative Corrections (RADCOR 98) World Scientific, 1998, Ed. J. Solà, pp 377-391 , [hep-ph/9903212](#).
- [15] J. A. Coarasa, J. Guasch and J. Solà, 4th Int. Symposium on Radiative Corrections, (RADCOR 98) World Scientific, 1998, Ed. J. Solà, pp 498-512 , [hep-ph/9903213](#).
- [16] J. A. Coarasa, J. Guasch and J. Solà, Physics at Run II: Workshop on Supersymmetry / Higgs, Fermilab 1998 , [hep-ph/9909397](#).
- [17] A. Belyaev, D. Garcia, J. Guasch and J. Solà, Phys. Rev. **D65**, 031701 (2002), [hep-ph/0105053](#).
- [18] A. Belyaev, D. Garcia, J. Guasch and J. Solà, JHEP **06**, 059 (2002), [hep-ph/0203031](#).
- [19] A. Belyaev, J. Guasch and J. Solà, Nucl. Phys. Proc. Suppl. **116**, 296 (2003), [hep-ph/0210253](#).
- [20] J. Guasch, W. Hollik and S. Peñaranda, Phys. Lett. **B515**, 367–374 (2001), [hep-ph/0106027](#).
- [21] J. Guasch, P. Häfliger and M. Spira, Phys. Rev. **D68**, 115001 (2003), [hep-ph/0305101](#).
- [22] M. Carena and H. E. Haber, Prog. Part. Nucl. Phys. **50**, 63–152 (2003), [hep-ph/0208209](#).
- [23] S. L. Glashow, J. Iliopoulos and L. Maiani, Phys. Rev. **D2**, 1285–1292 (1970).
- [24] S. Eidelman et al. (Particle Data Group Collaboration), Phys. Lett. **B592**, 1 (2004).
- [25] B. Mele, S. Petrarca and A. Soddu, Phys. Lett. **B435**, 401–406 (1998), [hep-ph/9805498](#).
- [26] S. Béjar, F. Dilmé, J. Guasch and J. Solà, JHEP **08**, 018 (2004), [hep-ph/0402188](#).
- [27] S. Béjar, J. Guasch and J. Solà, Nucl. Phys. **B675**, 270–288 (2003), [hep-ph/0307144](#).
- [28] S. Béjar, J. Guasch and J. Solà, Nucl. Phys. **B600**, 21–38 (2001), [hep-ph/0011091](#).
- [29] J. Guasch and J. Solà, Nucl. Phys. **B562**, 3–28 (1999), [hep-ph/9906268](#).
- [30] J. Guasch, in: proceedings of *Quantum effects in the minimal supersymmetric standard model*, pp. 256-265, World Scientific, 1998, ed. J. Solà , [hep-ph/9710267](#).

- [31] J. Guasch and J. Solà, in: proceedings of *4th International Workshop Detectors on Linear Colliders* (LCWS 99), Sitges, Barcelona, Spain, 28 Apr - 5 May 1999, pp.196-204, Universitat Autònoma de Barcelona, 2000, eds. E. Fernández, A. Pacheco , [hep-ph/9909503](#).
- [32] S. Béjar, J. Guasch and J. Solà, in: Proc. of the 5th International Symposium on Radiative Corrections (RADCOR 2000), Carmel, California, 11-15 Sep 2000 , [hep-ph/0101294](#).
- [33] A. M. Curiel, M. J. Herrero and D. Temes, Phys. Rev. **D67**, 075008 (2003), [hep-ph/0210335](#).
- [34] D. A. Demir, Phys. Lett. **B571**, 193–208 (2003), [hep-ph/0303249](#).
- [35] A. M. Curiel, M. J. Herrero, W. Hollik, F. Merz and S. Peñaranda, Phys. Rev. **D69**, 075009 (2004), [hep-ph/0312135](#).
- [36] S. Heinemeyer, W. Hollik, F. Merz and S. Peñaranda, Eur. Phys. J. **C37**, 481–493 (2004), [hep-ph/0403228](#).
- [37] A. Arhrib, Phys. Lett. **B612**, 263–274 (2005), [hep-ph/0409218](#).
- [38] J. A. Aguilar-Saavedra, Acta Phys. Polon. **B35**, 2695–2710 (2004), [hep-ph/0409342](#).
- [39] J. F. Gunion, H. E. Haber, G. L. Kane and S. Dawson, *The Higgs hunter’s guide*, Addison-Wesley, Menlo-Park, 1990.
- [40] M. S. Alam et al. (CLEO Collaboration), Phys. Rev. Lett. **74**, 2885–2889 (1995).
- [41] R. Barate et al. (ALEPH Collaboration), Phys. Lett. **B429**, 169–187 (1998).
- [42] S. Ahmed et al. (CLEO Collaboration), [hep-ex/9908022](#).
- [43] K. Abe et al. (Belle Collaboration), Phys. Lett. **B511**, 151–158 (2001), [hep-ex/0103042](#).
- [44] S. Chen et al. (CLEO Collaboration), Phys. Rev. Lett. **87**, 251807 (2001), [hep-ex/0108032](#).
- [45] B. Aubert et al. (BaBar Collaboration), 31st International Conference on High Energy Physics (ICHEP 2002), Amsterdam, The Netherlands, 24-31 Jul 2002 , [hep-ex/0207076](#).
- [46] S. Béjar, J. Guasch and J. Solà, in preparation .
- [47] M. Spira, HIGLU and HQQ packages: <http://people.web.psi.ch/~spira/higlu/>, and <http://people.web.psi.ch/~spira/hqq/>.

- [48] M. Spira, [hep-ph/9510347](#), HIGLU: A Program for the Calculation of the Total Higgs Production Cross Section at Hadron Colliders via Gluon Fusion including QCD Corrections.
- [49] M. Spira, A. Djouadi, D. Graudenz and P. M. Zerwas, Nucl. Phys. **B453**, 17–82 (1995), [hep-ph/9504378](#).
- [50] M. Spira, Fortsch. Phys. **46**, 203–284 (1998), [hep-ph/9705337](#), and references therein.
- [51] T. Hahn and M. Pérez-Victoria, Comput. Phys. Commun. **118**, 153 (1999), [hep-ph/9807565](#).
- [52] T. Hahn, *LoopTools* user’s guide, available from <http://www.feynarts.de/looptools>.
- [53] G. J. van Oldenborgh and J. A. M. Vermaseren, Z. Phys. **C46**, 425–438 (1990).
- [54] M. J. Duncan, Nucl. Phys. **B221**, 285 (1983).
- [55] A. Yamada, Z. Phys. **C61**, 247 (1994).
- [56] P. Chankowski, S. Pokorski and J. Rosiek, Nucl. Phys. **B423**, 437–496 (1994), [hep-ph/9303309](#).
- [57] A. Dabelstein, Z. Phys. **C67**, 495–512 (1995), [hep-ph/9409375](#).
- [58] A. Dabelstein, Nucl. Phys. **B456**, 25–56 (1995), [hep-ph/9503443](#).
- [59] M. Carena, S. Heinemeyer, C. E. M. Wagner and G. Weiglein, Eur. Phys. J. **C26**, 601–607 (2003), [hep-ph/0202167](#).
- [60] W.-Y. Keung and W. J. Marciano, Phys. Rev. **D30**, 248 (1984).
- [61] H. L. Lai et al. (CTEQ Collaboration), Phys. Rev. **D55**, 1280–1296 (1997), [hep-ph/9606399](#).
- [62] F. Gabbiani, E. Gabrielli, A. Masiero and L. Silvestrini, Nucl. Phys. **B477**, 321–352 (1996), [hep-ph/9604387](#).
- [63] M. Misiak, S. Pokorski and J. Rosiek, in “Heavy Flavours II”, eds. A.J. Buras, M. Lindner, Advanced Series on directions in High Energy Physics, World Scientific , [hep-ph/9703442](#).
- [64] O. Brein, Comput. Phys. Commun. **170**, 42–48 (2005), [hep-ph/0407340](#).
- [65] G. P. Lepage, J. Comput. Phys. **27**, 192 (1978).
- [66] M. Carena, S. Mrenna and C. E. M. Wagner, Phys. Rev. **D62**, 055008 (2000), [hep-ph/9907422](#).
- [67] S. Heinemeyer, W. Hollik and G. Weiglein, JHEP **06**, 009 (2000), [hep-ph/9909540](#).